TARGET RELATED MULTISPECTRAL AND TRUE COLOUR OPTIMIZATION OF THE COLOUR CHANNELS OF THE LH SYSTEMS ADS40

Ralf REULKE[*], Karl-Heinz FRANKE[**], Peter Fricker[***], Torsten POMIERSKI[**], Rainer Sandau[***], Maria von SCHÖNERMARK[*], Carmen TORNOW[*], Lorenz WIEST[*]

[*] German Aerospace Center DLR, Germany
Institute of Space Sensor Technology and Planetary Exploration
ralf.reulke@dlr.de

[**] Ilmenau Technical University, Germany
Faculty Computer Science and Automation
karl-heinz.franke@prakinf.tu-ilmenau.de,

[***]LH Systems GmbH, Switzerland
fricker@lh-systems.com, sandau@lh-systems.com

Working Group I/3

KEY WORDS: CCD, Scanner, High-Resolution Images, Multispectral Data, Data Fusion.

ABSTRACT

The LH Systems ADS40 airborne digital sensor is the first commercial digital CCD-line scanner for photogrammetric applications. CCD sensors allow true radiometric measurements in images. Multispectral channels, in addition to the stereo channels, can simply be incorporated together in one focal plane. Multispectral imagery with high spatial resolution opens new remote sensing capabilities. Data fusion between the channels and other sensors together with additional digital elevation models derived from panchromatic stereo data create new scientific opportunities. Besides multispectral applications, true colour images become more important for photogrammetric applications and are to be derived from colour processed multispectral images. When choosing multispectral bands narrow band filters on interesting spectral features are necessary. Therefore true colour images have to be derived from the multispectral channels. This paper shows an approach to fulfil both multispectral and true colour requirements.

1 INTRODUCTION

The ADS40 is the first commercial digital CCD-line scanner for photogrammetric applications. The main features of this digital airborne sensor are:

- High area coverage performance (FoV, swath)
- High resolution and accuracy (spatial and radiometric)
- Multispectral imagery
- Stereo capability
- Direct digital workflow
- Affordable, application oriented sensor.

Spectral band	TM (USA)	ATM (USA)	SPOT (France)	AVNIR (Japan)	Polder (France)	MOMS (Germany)	AVHRR (USA)	BIRD (Germany)	DPA (Germany)
Blue	0.45-0.52	0.42-0.45 0.45-0.52		0.42-0.5	0.42-0.46 P 0.42-0.46 0.47-0.51	0.44-0.505			0.44-0.525
Green	0.52-0.6	0.52-0.6	0.5-0.59	0.52-0.6	0.545-0.585	0.53-0.575			0.52-0.6
Red	0.63-0.69	0.605-0.625 0.63-0.69 0.695-0.75	0.61-0.68	0.61-0.69	0.65-0.69 P	0.645-0.68	0.55-0.68	0.6-0.67 F	0.61-0.685
NIR1	0.76-0.9	0.76-0.9	0.79-0.89	0.76-0.89	0.745-0.785 0.845-0.885	0.77-0.81	0.725-1.1	0.84-0.89 N 0.84-0.89 B	0.77-0.89
NIR2		0.91-1.05			0.89-0.93				

Table 1. Spectral channels of selected multispectral instruments (in the visible and near infrared spectral part)

In addition to multispectral applications, true colour images become more and more important for photogrammetric applications and are to be derived from colour processed multispectral images. Spectral position and spectral bandwidth of both multispectral and true colour imagery are different. Multispectral applications need non-overlapping narrow bands and an infrared channel close to the vegetation red edge, whereas true colour channels are closely related to the eye's sensitivity and therefore require broad band overlapping channels. The main focus of the spectral optimisation of the colour channels lies therefore on the multispectral applications. True colour images are derived from multispectral channels afterwards. Table 1 lists spectral channels of spaceborne and airborne multispectral instruments.

The optimisation of the multispectral channels can only be achieved with dedicated applications. The channels are selected by focussing on classification and information content for different vegetation types, bare soils and sealed areas. Simulations also show that the wavelength range of the panchromatic channel must be related to the multispectral channels. Therefore only small changes in the spectral position and bandwidth are possible for the optimisation of the true colour channels. To generate true colour from multispectral channels an optimal transformation is used with three colours and, if necessary, an additional panchromatic channel. The transformation parameters must be related to future applications of the airborne scanner. This restricts colour space.

2 ADS40

The LH Systems ADS40 digital sensor is the next generation digital sensor for airborne photogrammetry and remote sensing. The ADS40 has a modular customised concept with three panchromatic and four multispectral CCD lines. The three panchromatic sensor lines produce the forward, nadir and backward views along the strip. Each panchromatic line consists of two linear arrays, each with 12000 pixels, staggered by 0.5 pixels. Each sensor line is measured during camera calibration so that the precise position of each pixel on the focal plane is known.

2.1 Design criteria for multispectral systems

The number of channels desirable in a given spectral region depends on their half-width, which limits on the one hand the signal-to-noise ratio and the energy reaching the detector. But on the other hand the larger the number of channels used the better defined is the information measured. This describes the situation of a typical optical spectrometer. Because of the limited energy, spectrometers with high spectral resolution cannot reach fine spatial resolution. The ADS40, however, is tailored above all to photogrammetric tasks and needs a very fine spatial resolution. Hence, the channel width should not be smaller than 50 nm. With this assumption four or a maximum of five channels provide the maximum information. Some of the tasks given below require corrections to the data sets (atmospheric correction, correction with respect to the viewing angles, BRDF effects) or a suitable geoinformation system.

2.2 Design criteria for true colour systems

As mentioned above it is impossible to derive an overall approach to transform multispectral to true colour images. Therefore a restriction on the future tasks of this sensor-system is necessary. The optimisation criterion during the derivation of the transformation parameters is the colour impression of imaged objects. For that purpose 65 spectral surface reflectances β_i where selected from the NASA-Reference (1985), hereafter referred to as "the NASA reflectances". The influence of the atmosphere on the colour impression was simulated with a standard atmospheric model (MODTRAN 3.5). During simulations several parameters - flight altitude, illumination, extinction and aerosol type - were changed. To fill the whole colour space an additional standard colour test set (DIN 6169 part 7) was used. This approach allows the fine tuning of the spectral channels and the derivation of transformation parameters for true colour representation.

3 SELECTION OF THE SPECTRAL CHANNELS

The combination of the channels depends on the object that is going to be investigated and the task to be performed. The following tasks are identified:

1. Presentation in true colours is preferred in order to
   - observe and document the surface
   - map out land use
   - eliminate cloudy areas
   - locate ice sheets in water areas.

   It is also desirable to use the blue channel, because in this wavelength range the scattering by air particles is very high, which allows the sensor to receive information from the shadowed areas. Mapping of land use and documentation of the development of landscape is required by government ministries and authorities (for example planning departments for traffic or urban development, protection of nature and the environment). By using this

channel combination the extent and damage of natural disasters or coastal erosion can be detected. The surface roughness as well as the sensible and latent heat flux resistances are usually derived from land use maps.

2. For cloud investigations two or three channels (blue and green and in addition sometimes red) are routinely used. In the blue channel clouds can be well detected and it is used for spatial analyses of cloud structure.
3. Monitoring of water areas can also be done with two or three channels: the ratio of the blue and the green channel, or the two channels separately, is used for testing lakes with regard to water quality and algae. For detecting oil spills one channel in the blue region and another one in the NIR region between approximately 760 and 780 nm are desirable. (But it should be mentioned that an active microwave system is more suitable for carrying out this task.)
4. For monitoring vegetation and deriving plant parameters three channels are often used (green, red and NIR). However, many tasks can be performed with two channels in the red and NIR region. Measurements in these channels, repeated several times during a season, give information about natural, anthropogenic or climatic induced effects on the biosphere. Typical tasks are the retrieval of phenological parameters and the determination of vegetation indices, leaf area index (LAI) and the absorbed photosynthetically active radiation. With these parameters the biomass, which is produced or destroyed within the time period investigated, can be estimated and hence the crop yield and the amount of carbon dioxide, which is fixed as carbon in the biomass produced, can be calculated by models. This last parameter is highly essential in all investigations of climate variability. The plant parameters mentioned above are often used for estimating evapotranspiration. In addition the proposed channels allow the identification of changes in the vegetation, such as forest damage as well as stress on drylands, and to the issuing of early warnings about possible food shortages. Using the red and NIR channels different vegetation types can be classified (Hahn, 1996). This is interesting for planning offices, agricultural establishments, and institutions and ministries dealing with the protection of biotops, species and diversities.

3.1 Selection of Channels

The spectral surface reflectance and the atmospheric transmittance within the spectral region from 400 nm to 1000 nm is shown in Figure 1. In the left part of the figure the transmittance of the atmosphere due to the uniform mixed gases and a typical (averaged) transmittance value of the variable constituents of ozone and water vapour is depicted. In order to avoid the reduction of the surface signal due to atmospheric absorption, the channels should be positioned within atmospheric windows. These are the regions where only minor absorption by the atmospheric constituents occurs. In the right part of the figure typical spectra of surface reflectances as well as the reflectances of two different types of cloud components are presented.

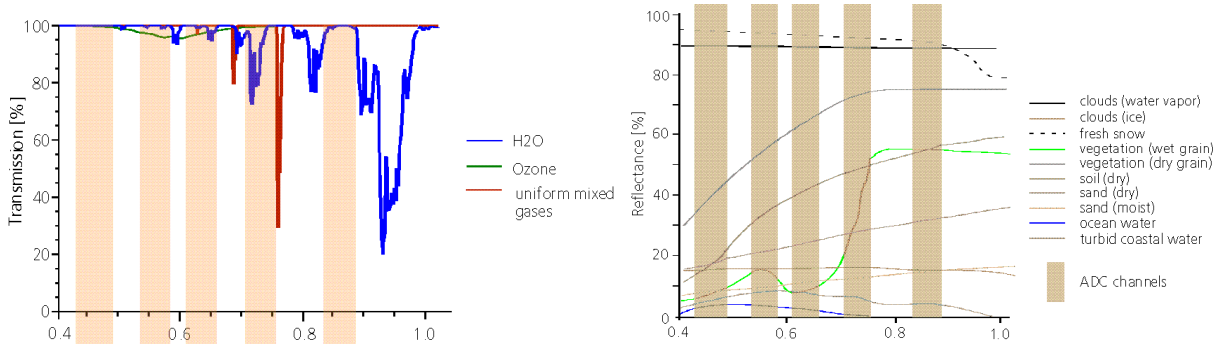

Figure 1. ADS40 spectral bands. Atmospheric absorption bands (left) and typical spectral reflectances (right)

The following channels have been selected for the ADS40:

- channel 1 - blue: 460nm +/-30 nm. The weak chlorophyll absorption band of green vegetation in water areas or at the surface (maximum between 430 and 450 nm) is located in this spectral region. This absorption band is important when using this channel for monitoring water areas.
- channel 2 - green: 560 nm +/-25 nm. This spectral domain is characterised by the reflectance maximum of the green vegetation and is of some importance for the detection of chlorophyll in water areas.
- channel 3 - red: 635 nm +/- 25 nm. The second chlorophyll absorption band (maximum : 650 nm) is located in this region. The selection of the red channel is also determined by the condition that the long-wave side of the red channel should break off in concordance with the panchromatic channel at 700 nm.
- channel 4 - NIR: 730 nm +/-25 nm. The oxygen-band is situated at the long-wave side of this channel. Since the oxygen concentration is known and is constant in space and time, it can be taken into account in the software algorithm. For low flight altitudes it can even be neglected. Unfortunately, the weak water vapour band centred at 720 nm reaches into the proposed channel. This is inevitable, because the water vapour is above all concentrated in the lower part of the atmosphere and has a high variability in space and time. On the other hand this channel is required for identifying vegetation. The channel is located in the strong rise (red edge) of the reflectance curve for green vegetation

- channel 5 - NIR: 870 nm +/-35 nm. The disadvantage of this channel is the wide shape of the point spread function. Hence, the spatial resolution in this channel is no longer the same as in the red one. But this channel is necessary for some applications in retrieving plant parameters. Hence it follows that over heterogeneous areas channel 4 should be used instead of channel 5.

Table 2. summarises the values for the selected channels and their main characteristics for the user.

Channel	Centre Wavelength λ_0 [nm]	Tolerance $\Delta\lambda_0$ [nm]	FWHM at T = 50% [nm]	Comments	Characteristics
Blue	460	±10	60	Pure CCD sensitivity	water (maximum absorption) maximum light scattering oil (with NIR) RGB
Green	560	±5	50		water, vegetation (green reflectance peak) RGB
Red	635	±5	50		discrimination of vegetation (with NIR) RGB
NIR 1	730	±5	50	Balance between H_2O_D + CCD Broad PSF	discrimination of vegetation determination of biomass vegetation - state of health mapping shorelines discrimination of vegetation and soil pavement PSF (Point Spread Function)
NIR 2	860	±10	50	Broad PSF	

Table 2. Selected channels and their main characteristics

3.2 Signal-to-noise ratio (SNR) – calculation for ADS40 spectral channels

This calculation is mainly focused on the signal in relation to the camera and Poisson noise. In this case the signal estimation can be reduced on the calculation of the number of generated electrons.

$$n = \tau_{\text{int}} \cdot \frac{\pi}{4k^2} \cdot \cos^{\kappa}\theta \cdot \int_{\lambda_0}^{\lambda_1} d\lambda\, R(\lambda) \cdot T(\lambda) \cdot L(\lambda) \qquad (1)$$

L is the radiance in front of the sensor, τ_{int} the integration time (1 ms), k the f/# of the optics, $\cos^{\kappa}\theta$ the shading of the optical system, T the transmittance of the optical system and R the responsivity of the detector element. The calculation was made with the following parameters. The detector size is A=6.5∗6.5 μm^2. The spectral range is defined by table 2. The ADS40 optics have an f/# = 4. The noise of the electrical channel in electrons is rms=150 e^-. The radiance in front of the sensor was calculated with the 6S program (Vermote, 1996). The results are obtained with a mid-latitude summer model, an urban aerosol model, visibility 23 km, solar zenith angle 30°, and nadir view angle. Test targets are vegetation, sand and lake water. Table 3 shows the results of the calculation. The calculation indicates a reasonable signal to noise ratio for all spectral channels.

Centre Wavelength	FWHM	Vegetation	SNR	Sand	SNR	Water	SNR
0.46	0.06	7504	43	8055	46	6526	38
0.56	0.05	8547	48	9191	51	6307	37
0.635	0.05	5770	34	11369	61	5576	33
0.73	0.05	27332	122	14122	73	3242	20
0.86	0.05	31147	134	17068	85	1585	10
PAN		94567	276	81490	252	41458	163

Table 3. Generated electrons and SNR for different test targets

4 SELECTION OF THE TRUE COLOUR CHANNELS

4.1 Human colour perception

The colour values $\underline{\mathbf{F}} = \{ R, G, B \}^T$ describe human colour perception with regard to a colour synthesis system and are ultimately defined by the comparison method.
Historically, as the first colorimetric interface, the RGB-CIE coordinates are based on three narrow-band stimuli (10 nm) at 700 nm (R), 500 nm (B), and 400 nm (B). Because technical colour synthesis systems (i.e. in colour televisions and monitors) are based on the spectral emissions of phosphors, modified colorimetric interfaces are relevant. In Europe, this interface corresponds to the EBU norm (European Broadcasting Union) for so called EBU phosphors. For every colour stimulus $\varphi(\lambda)$, a synthesised emission must be generated by weighting of the normalised spectral densities from the EBU phosphor $p_R(\lambda)$. This spectral density is according to the sensitivity of the cones in the human eye (p,d,t),

$$\underline{z} = \{z_1, z_2, z_3\}^T = \{\bar{p}, \bar{d}, \bar{t}\}^T \tag{2}$$

and leads to the identical colour sensation $\underline{\mathbf{F}}$ as in the case of the stimulus $\varphi(\lambda)$.

$$\int_{380nm}^{780nm} d\lambda \; z_i(\lambda)\, \varphi(\lambda) = \int_{380nm}^{780nm} d\lambda \; z_i(\lambda) \; [R \; p_R(\lambda) \quad + G \; p_G(\lambda) \quad + R \; p_B(\lambda)] \tag{3}$$

A true-colour camera gives these RGB weights.

$$\underline{F} = \{R, G, B\}^T = k \int_{\lambda} d\lambda \; \varphi(\lambda)\, \underline{s}(\lambda) \tag{4}$$

$\underline{s} = \{s_1, s_2, s_3\}^T$ is the overall sensitivity of the three camera channels. Substituting (4) into (3), and considering narrow-band emissions $\varphi(\lambda) = \delta(\lambda-\lambda_0)$

$$k \int_{\lambda} d\lambda \;\; \delta(\lambda - \lambda_0)\, \underline{s}(\lambda) = k \; \underline{s}(\lambda_0) \;\text{ and }\; \int_{380nm}^{780nm} d\lambda \; z_i(\lambda)\, \delta(\lambda - \lambda_o) = z_i(\lambda_0) \tag{5}$$

leads to the system of linear equations to determine the necessary sensitivity of the three sensor channels at λ_0.

$$\underline{z}(\lambda_0) = \left[\int_{380nm}^{780nm} d\lambda \;\; \underline{z}(\lambda)\, \underline{p}^T(\lambda) \right] k \; \underline{s}(\lambda_0) \tag{6}$$

The variation of $\lambda_0 \left(\lambda_0 \in [380\text{nm}, 780\text{nm}]\right)$ gives the spectral values curve of the EBU phosphor,

$$\underline{s}(\lambda) = \{s_1(\lambda), s_2(\lambda), s_3(\lambda)\}^T = \{\bar{r}(\lambda), \bar{g}(\lambda), \bar{b}(\lambda)\}^T \tag{7}$$

which, as the overall sensor sensitivity, must be obtained for true-colour cameras (including negative portions). With the uniform sensitivity $s(\lambda)$ of the sensor material and the Luther condition

$$\underline{s}(\lambda) = \underline{s}^*(\lambda) \cdot s(\lambda) \tag{8}$$

the required filter curves $\underline{s}^*(\lambda)$ (along with their negative portions) can be separated. In colour cameras, these technologically achievable transmission functions are approximated by implementable filter curves, with the help of linear transformations:

$$\underline{s}^*(\lambda) = \underline{\underline{T}} \cdot s_C^*(\lambda) \tag{9}$$

Requirements for this are three wide-band filter curves with different band centres, and sufficient overlap, so that the entire visual spectrum is covered.

4.2 Optimization based on an overall sensor sensitivity

The approximation of true colour under conditions of given remote sensing channels shall be now investigated in terms of the overall sensor sensitivity. Three spectral channels are available, in the short, medium, and long wave ranges of the visual spectrum,

$$\underline{s}_s(\lambda) = \{s_l(\lambda), s_m(\lambda), s_k(\lambda)\}^T \tag{10}$$

as well as one panchromatic channel $s_p(\lambda)$, which nearly covers the entire visual spectrum.

$$\underline{s}_{ADC}(\lambda) = \{s_l(\lambda), s_m(\lambda), s_k(\lambda), s_p(\lambda) \;\}^T \tag{11}$$

Taking into account the superposition principle [assumed in equation (2) and applicable in the case of the human eye (retinal cavity)], a good approximation of the spectral values curve should be optimal for all colour emissions. The quality function for minimising the mean square errors (MSE) is determined by:

$$Q_\lambda = \sum_i \left(\underline{s}(\lambda_i) - \underline{\underline{M}}_\lambda \, \underline{s}_{ADC}(\lambda_i)\right)^T \left(\underline{s}(\lambda_i) - \underline{\underline{M}}_\lambda \, \underline{s}_{ADC}(\lambda_i)\right) \tag{12}$$

with $\lambda_i = 380nm + i\,\Delta\lambda$ and $\Delta\lambda = 10nm$.

Owing to restrictions in $\underline{s}_{ADS40}$, the 4 x 3 matrix $\underline{\underline{M}}$ (curve with open squares in figure 2) insufficiently represents the spectral curve (curve with filled squares). A target-independent solution can therefore not be expected. In addition to the spectral values in figure 1, the colour coordinates of the 17 DIN test colours (filled squares) and the representation achievable by the transformation with $\underline{\underline{M}}$ for D_{65} lighting (open squares) is shown. These statements can be quantitatively corroborated by observing aerial pictures of the target.
The mean Euclidian distance in the used colour space ΔE has values of 6.09 for the DIN test colours and 3.89 for the NASA reflectances under D_{65} lighting conditions near ground level.

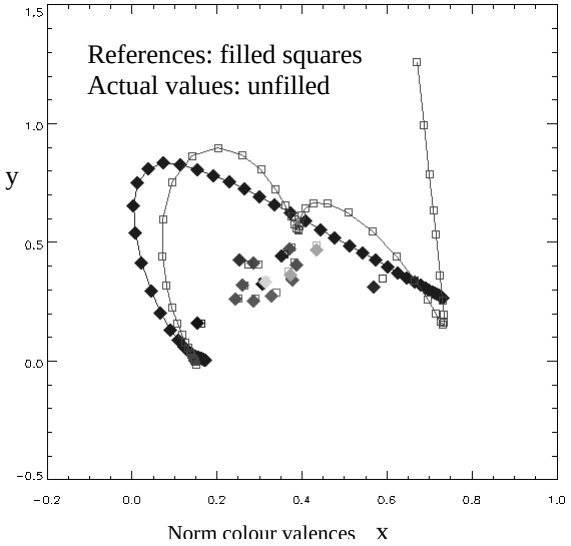

Figure 2. Spectral MSE approximation

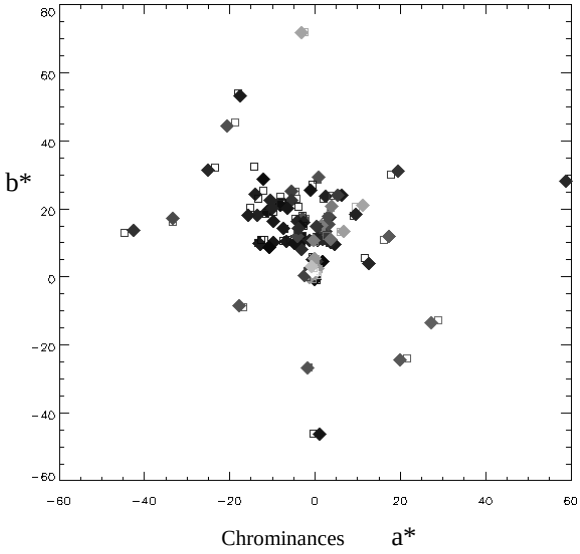

Figure 3. Target related calibration

4.3 Optimization of Colour Values of the Expected Target

Better results can be achieved in reference to the colour values of the expected target (including integration of the 17 DIN test colours).

$$Q_T = \sum_{i=1}^{N} \left(\underline{F}_{i\,ref} - \underline{\underline{M}}_T \, \underline{F}_{i\,actual}\right)^T \cdot \left(\underline{F}_{i\,ref} - \underline{\underline{M}}_T \, \underline{F}_{i\,actual}\right) \tag{13}$$

(N: 65 colour coordinates from NASA reflectances and 17 DIN test colours). Initially, near ground level and D_{65} lighting were focused on:

$$F_{i\,ref} = k \sum_\lambda D_{65}(\lambda)\, \underline{s}(\lambda)\, \beta_i(\lambda) = \{R_i, G_i, B_i\}^T \tag{14}$$

$$F_{i\,actual} = k \sum_\lambda D_{65}(\lambda)\, \underline{s}_{ADC}(\lambda)\, \beta_i(\lambda) = \{L_i, M_i, K_i, P_i\}^T \tag{15}$$

By omitting the panchromatic channel [i.e. by using $\underline{s}_s(\lambda)$ instead of $\underline{s}_{ADS40}(\lambda)$] and omitting P_i in equation (14), median deviations of ΔE = 5.86 (DIN) and ΔE = 2.41 (NASA) were determined. At least for the test colours, these values lie well above the perceptible threshold of ΔE = 3.0. Because these values are median deviations, perceptible differences must also be expected for the NASA reflectances. By taking into account the panchromatic channel in equation (14), the results are significantly better (ΔE = 2.31 (DIN), ΔE = 1.47 (NASA)). Optimising the band centres of the spectral channels using adaptive stochastics, within the limits of the allowed degrees of freedom, brings results of ΔE = 1.39 and ΔE = 1.14 (figure 3). The variation of additional parameters (top width and slope of the panchromatic channel) did not yield significant improvements.

The solution $\underline{\underline{M}}_T$, based on the 65 NASA reflectances for D_{65} lighting, was validated with an additional 31 NASA reflectances and led to a very good result of ΔE = 0.99. In real applications of this type of camera, when the concrete recording conditions are taken into account, significant changes in the colour emissions at constant target reflectance must be expected. This pertains not only to intensity, but also the colour locations of the targets. Experience has shown

that increasing flight altitude and decreasing visibility is connected with a strong desaturation of all colour values. This effect was investigated, with the goal of evaluating the stability of the quality of the approximation when using the determined transformation matrix $\underline{\underline{M}}_T$.
For this purpose, the D65 recording conditions were replaced by approximated real radiation contributions from a data cube (figure 4).

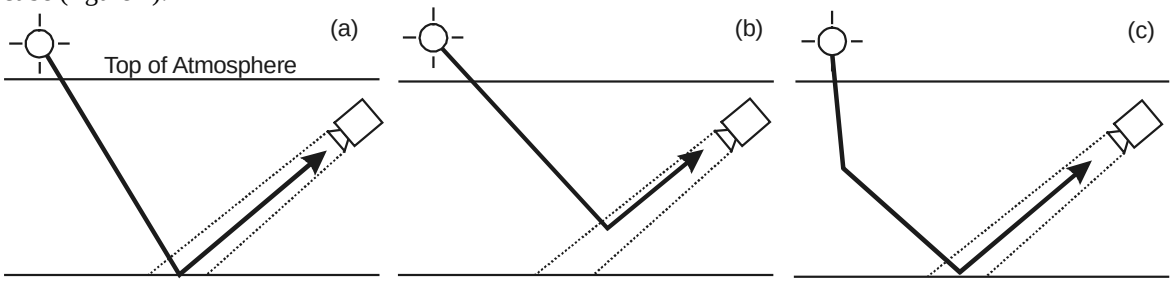

Figure 4. Radiance contributions to the total at-sensor radiance as stored in the data cube to approximate real radiation conditions. From left to right: (a) direct reflected radiance, (b) solar scattered path radiance, (c) diffuse solar radiance

This data cube consists of a set of spectral look up tables which were created by processing the output results (tape7) of the radiation transfer code MODTRAN 3.5. The use of such a data cube saves computing time by avoiding re-runs of MODTRAN 3.5 for each iteration of the optimisation. Each look up table is connected to a particular input parameter tuple of MODTRAN such as sensor orientation, aerosol type, visibility, sensor altitude, ground altitude, and the sun's zenith angle. By having a set of such look up tables available, the influence of the variation of these parameters on the optimization can be taken into consideration.

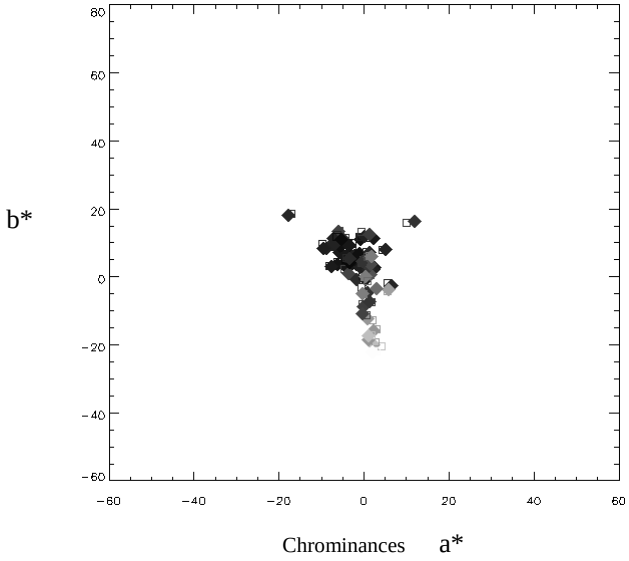

Figure 5. Influence of flight and environmental data

With this modified lighting source, sensor orientation, aerosol type, visibility, sensor height, ground height and the sun's zenith angle can be varied and taken into consideration. Figure 5 shows the expected basic influences. In addition to desaturation, increasing damping in the long wave VIS range (present under all real recording conditions) leads to a shifting of the colour coordinates towards blue. With a ΔE of circa 1.15, the solution proved to be robust enough, so that an optimisation based on the flight parameters was unnecessary.

4.4 Non-linear Adjustment

An even better approximation of the expected target values can be achieved through a non-linear approach with respect to the actual values of the ADS40 channels, in the simplest case, by adding quadratic terms [ΔE = 1.56 (test colours) and 1.38 (NASA targets) as against 2.31 and 1.48, with no changes in the filter curve]. However, the improved approximation of the targets by non-linear approaches sometimes leads to an extreme distortion of the colour space between targets. Additionally, the approximation of the chromacity value becomes strongly dependent on brightness. If changes in the recording conditions occur, or additional reflectances not used in the optimisation appear, extreme deviations in colour values can be expected.

4.5 Differentiation and Data Spread

The good approximation of the target values on the average still leaves important questions open. On the one hand, it should be investigated whether target values that can be differentiated visually can still be differentiated in the camera image. Owing to the linearity of the transformation, checking critical colour differences (i.e. the smallest colour difference) between target pairs should be sufficient.

Target A	Target B	Δ E EBU	Δ E ADS40
Yellow Corn	Wheat	2.11	3.30
Flax	Birch Leaves	3.93	2.91
Oats	Tomatoes	3.13	2.93
Unaltered Rocks	Quartz Beach Sand	3.23	2.31
Altocumulus Clouds	Wet Snow	2.11	2.44

Table 4. Selected results

The target pairs shown in the table are characteristic for these critical cases and show that the magnitude of colour spacings is maintained. The critical cases often pertain to colour values of target pairs that, through the perception of colour only, cannot be differentiated even with the eye. Overall, it is not expected that the ability to differentiate is

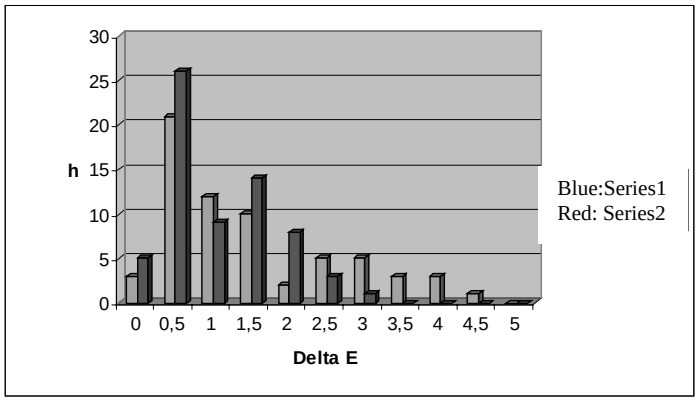

Figure 6. Spread of ΔE

impacted.

On the other hand, even for good average ΔE values, it must be proven that the maximum single deviation remains below the visual perception threshold. The histogram analysis of colour deviation between visual perception and camera image shows three reflectances with $\Delta E = 3.5$, 3 with $\Delta E = 4$, and one with $\Delta E = 4.5$ (figure 6, blue). Thus, the critical cases lie above the visual perception threshold. This is the case for unchanged filter parameters. However, optimisation of the band centres in the spectral channels through adaptive stochastics (within the limits tolerated by remote sensing) and simultaneous widening of the top width in the panchromatic channel lead to maximum individual deviations of all target values, E_{max}, below three (figure 6, red).

5 CONCLUSIONS

This paper shows a physical and task related approach for deriving spectral channels for multispectral and true colour systems. The multispectral channels are fixed in accordance with the problem to be solved from a scientific standpoint and true colour images must be derived from this channels by colour transformation. To improve the appearance of the true colour image, the panchromatic channel can be used.

REFERENCES

Bowker, D.E., Davis, R.E., Myrik, D.L., Stacy, D.L., 1985. Spectral Reflectances of Natural Targets for Use in Remote Sensing Studies. NASA-Reference-Publication 1139.

Franke, K.-H., Pomierski, T., Reulke, P., 1999. Targetbezogene True-Colour-Kalibrierung, 5. Workshop Farbbildverarbeitung, Proceedings, Schriftenreihe des ZBS, Report Nr. 1/99, Ilmenau, FRG

Hahn, F., 1996. The discrimination integration index as a broadband discrimination index. SPIE 2818, pp. 95-103.

Vermote, E., Tanre, D., Deuze, J.L., Herman, M., Morcrette, J.J., 1996. Second simulation of the satellite signal in the solar spectrum (6S). NASA Goddard Space Flight Center for Medium Range Forecast.